Theoretical Studies on Low-Lying Electronic States of Cyanocarbene HCCN and Its Ionic States

Zeng-Xia Zhao, Hong-Xing Zhang,* and Chia-Chung Sun

Institute of Theoretical Chemistry, State Key Laboratory of Theoretical and Computational Chemistry, Jilin University, Changchun 130023, People's Republic of China

Received: August 7, 2008; Revised Manuscript Received: September 23, 2008

Geometries of 10, 7, and 6 low-lying states of the HCCN neutral radical, its anion and cation, were optimized by using the complete active space self-consistent field (CASSCF) method in conjunction with the aug-cc-pVTZ basis set, respectively. Taking the further correlation effects into account, the second-order perturbations (CASPT2) were carried out for the energetic correction. Vertical excitation energies (T_v) at the ground state geometry of the HCCN neutral radical were calculated for 11 states. The results of our calculations suggest that the spin-allowed transitions of HCCN at 4.179, 4.395, 4.579, 4.727 and 5.506 eV can be attributed to $X^3A'' \rightarrow 2^3A''$, $X^3A'' \rightarrow {}^3A'$, $X^3A \rightarrow 3^3A''$, $X^3A'' \rightarrow 2^3A'$, and $X^3A'' \rightarrow 3^3A'$, respectively. The singlet−triplet splitting gap of HCCN is calculated to be 0.738 eV. The vertical and adiabatic ionization energies were obtained to compare with the PES data. The results we obtained were consistent with the available experiment results.

Introduction

Both experimental and theoretical researches have had a long-standing interest in the chemistry of carbenes especially in their applications in chemical reactions.[1,2] Cyanocarbene, HCCN, is a cyano derivative of the simplest carbene, CH_2, and is an important interstellar molecule that is thought to be an intermediate in formation of larger polynitriles.[3,4] The equilibrium structure and spectroscopic properties of HCCN have been the subject of a series of researches.[5−32] Initial experimental studies in low-temperature matrices using ESR, IR, and UV spectroscopy concluded that HCCN was linear in its $^3\Sigma^-$ ground state,[5−8] and Dendramis and Leroi[7] suggested for the ground state the allenic structure H−•C═C═•N. In 1984, the ground state of HCCN was characterized by Saito et al.,[8] who measured several low-*J* rotational transitions by microwave spectroscopy. They saw no deviation in the spectrum from the expectations for a linear molecule in an Σ state and so, in agreement with earlier experimental observations, they concluded that HCCN is a linear radical. A more thorough microwave study was conducted by Brown et al.,[9] who measured the pure rotational spectrum of four isotopomers and were able to determine the substituted structure. They found an anomalously short internuclear distance (0.998 Å) for the C−H separation and concluded, for the first time, that HCCN is quasilinear instead of strictly linear. Furthermore, a high-resolution study of the ν_1 CH stretch by Morter et al.[10] and a millimeter wavelength study of the pure rotational transitions by McCarthy et al.[11] both found several low-lying HCC bending vibrational states, which were evidence for quasilinearity. In a series of high-resolution infrared studies,[12−15] Curl and co-workers proposed a quasilinear structure based on measurements of the ν_5 bending vibrational frequency.

On the theoretical side, virtually all theoretical researches since the late 1970s suggest that the bent cyanocarbene

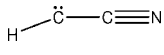

is the lowest energy structure.[16−32] In 1982, Kim et al.[19] calculated that the bent HCCN structure was 700 cm^{-1} more stable than the linear configuration and labeled the molecule quasilinear. Subsequent calculations continued to maintain the greater stability of the bent HCCN structure, but the barrier to linearity decreased with increasing sophistication of ab initio theory and larger basis sets. In CCSD(T) calculations from Schaefer's group,[24] the linear structure HCCN($^3\Sigma^-$) was predicted to lie only ∼277 cm^{-1} higher above the bent conformation ($^3A''$). This value is consistent with their previous studies,[18,22] as well as those of Malmquist et al.,[21] Aoki et al.,[23] and Koput.[28] Other theoretical studies have focused on the thermochemical properties and singlet−triplet splitting for HCCN.[23−32]

However, the electronic spectroscopy of the HCCN radical is currently not well characterized. Only Aoki et al.[23] report ab initio calculations for the two low-lying excited electronic states of HCCN. Vertical transition energies from the X^3A'' ground state to $^1A'$ and $^1A''$ excited states were found to be 0.93 and 1.11 eV, respectively.

In 2002, Nimlos et al.[29] observed the PES of the $HCCN^-$ anion; they measured the electron affinity of cyanocarbene to be 2.003 ± 0.014 eV for the triplet state, implying a heat of formation of 110 ± 4 kcal/mol and a triplet−singlet splitting of 11.9 ± 0.3 kcal/mol, which is in good agreement with theoretical predications. However, there were only a few studies on the $HCCN^-$ anion.[25,29,32] The electronic ground state X^2A'' and excited state $^2A'$ of $HCCN^-$ have been investigated with different methods but the other excited states have not been studied. There was only a little theoretical work on cationic [H, C_2, N] potential energy surface,[25] whereas there has not been experimental or theoretical reports on the characters of the excited states of $HCCN^+$.

It is well-known that the CASPT2 and CASSCF methods are effective for theoretical studies of excited states of molecules. The aim of this work is to study a large number of electronic states of the HCCN radical and its ions $HCCN^-$ and $HCCN^+$ by using the CASPT2//CASSCF method. We report the results for excited electronic states, including the predicted equilibrium geometries, harmonic vibrational frequencies, and adiabatic and vertical excitation energies.

* Address correspondence to this author.

10.1021/jp8070663 CCC: $40.75
Published on Web 10/30/2008

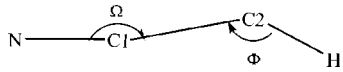

Figure 1. Sketch of the molecular geometries of the HCCN and definition of the bond angles Ω and Φ.

Calculation Methods

The electronic structures of the HCCN neutral radical and its ionic states were investigated using the complete-active-space self-consistent field (CASSCF) level of theory. Multiconfigurational linear response (MCLR) was used to calculate the harmonic frequencies, and complete-active-space second-order perturbation (CASPT2) was used to calculate the dynamic correlation. The calculations were performed by using the augmented correlation consistent valence triple-ζ aug-cc-pVTZ basis sets. According to the CASPT2 energies calculated at the respective geometries optimized at the CASSCF level, we obtained the CASPT2//CASSCF/aug-cc-pVTZ adiabatic excitation energy values.

Geometries and atom labelings used for HCCN, $HCCN^-$, and $HCCN^+$ are shown in Figure 1. We assume that HCCN, $HCCN^-$, and $HCCN^+$ in all the studied electronic states have planar C_s symmetry structure. In the CASSCF and CASPT2 calculations, the reference wave function consisted of a full-valence complete active space. Thus, the wave function included all excitations of 14 valence electrons in 13 molecular orbitals, corresponding to the valence atomic sp orbitals of the C and N atoms and the 1s orbital of the H atom, namely, ten a′ orbitals and three a″ orbitals. The same active orbitals were chosen for its anion $HCCN^-$ and cation $HCCN^+$, but the active electrons were increased or decreased by one, respectively. The geometries of all the states were optimized under C_s symmetry at the CASSCF level. The oscillator strength is defined as $f = 2(\mathrm{TDM})^2\Delta E/3$. The transition moments (TDM) were computed by CASSCF, and the excitation energies, which are very sensitive to dynamic correlation, were computed by CASPT2.

The four forms of neutral-ion energy differences reported were evaluated as differences of total energies: the adiabatic ionization potential, $\mathrm{IP_{ad}} = E$(optimized cation) − E(optimized neutral); the vertical ionization potential, $\mathrm{IP_{vert}} = E$(cation at optimized neutral geometry) − E(optimized neutral); the adiabatic detachment energy of the anion, ADE = E(optimized neutral) − E(optimized anion); and the vertical detachment energy of the anion, VDE = E(neutral at optimized anion geometry) − E(optimized anion).

The calculated energies are obtained from the calculations of the CASPT2//CASSCF level. All of the calculations were performed with the MOLCAS 6.0 quantum chemistry software[33] on SGI/O38600 and SGI/O3900 servers.

Results and Discussion

Equilibrium Geometries of the Ground State and Excited States of HCCN. The equilibrium geometries of the ground state and 9 low-lying excited states with C_s symmetry were obtained at the CASPT2//CASSCF level and summarized in Table 1, which also contains energies and electronic configurations. Comparing the energetic values of CASSCF and CASPT2 indicated the dynamical electron correlation effect must be considered in calculations. At both CASPT2 and CASSCF levels of theory, the X^3A'' state of HCCN is predicted to be the ground electronic state. The equilibrium geometry parameters calculated at the CASSCF level are $R_{CH} = 1.063$ Å, $R_{CC} = 1.372$ Å, $R_{CN} = 1.184$ Å, Ω = 175.6°, and Φ = 137.5°, which agrees well with previous theoretical calculations.[28−32]

The leading configurations of the CASSCF wave functions for the 10 states of HCCN were listed in Table 1. As shown in Table 1, the absolute values of the CI coefficient for the X^3A'', $^1A'$, $^1A''$, $2^1\Sigma^+(2^1A')$, $^3A'$, and $3^1A''$ of the HCCN leading configurations are above 0.90, indicating a single-reference character of the respective states. The value of the $2^3A''$ is 0.821, which indicates a low multireference character. The other states show obvious multireference characters. It seems that the high excited states tend to show multireference character. The electronic configuration of the ground state X^3A'' of HCCN can be described as $[\mathrm{core}](4a')^2(5a')^2(6a')^2(7a')^2(8a')^2(1a'')^2(9a')^\alpha(2a'')^\alpha$ where [core] represents $(1a')^2(2a')^2(3a')^2$. From the plots of the electronic density shown in Figure 2, we can see that the two single electrons of ground state X^3A'' reside in the 9a′ and 2a″ molecular orbital. The 9a′ shows mainly dominant n_{xy} (C: $2sp_xp_y$) nonbonding character and little π^*(C2−N) (C2−N antibonding) contributions from the N atom. Likewise in the 2a″ orbital, it has mainly n_z (C: $2p_z$) nonbonding character with little antibonding contribution (π^*(C2−N)).

The single-electron transition 2a″ → 9a′ results in the first excited state $^1A'$, which has a dominant leading configuration $[\mathrm{core}](4a')^2(5a')^2(6a')^2(7a')^2(8a')^2(1a'')^2(9a')^2(2a'')^0$ with a coefficient of 0.930. The geometrical parameters of this state are $R_{CH} = 1.114$ Å, $R_{CC} = 1.413$ Å, $R_{CN} = 1.173$ Å, Ω = 174.1°, and Φ = 107.6°, which are consistent with the $R_{CH} = 1.106$ Å, $R_{CC} = 1.410$ Å, $R_{CN} = 1.177$ Å, Ω = 172.8°, and Φ = 107.1° calculated at the QCISD/6-311G(d,p) level.[29] The singlet−triplet splitting energy of HCCN has been found experimentally to be 11.1 ± 5.8 kcal/mol,[30] which is in very good agreement with our value of 17.0 kcal/mol (0.738 eV). The triplet−singlet energy difference for HCCN is predicted to be slightly larger than that for the parent CH_2 carbene, 0.392 ± 0.002 eV.[34−38]

The state $^1A''$ has the leading configuration $[\mathrm{core}](4a')^2(5a')^2(6a')^2(7a')^2(8a')^2(1a'')^2(9a')^\alpha(2a'')^\beta$ with a coefficient of −0.940, in which the two single electrons are antiparallel spin. Compared with the ground state, R_{CC} is shortened 0.053 Å, R_{CN} is elongated 0.019 Å, the R_{CH} is shortened 0.006 Å, the angle Ω is increased 0.6°, and the angle Φ is increased 18.1°.

The largest bond angle Φ appears in the $2^1\Sigma^+(2^1A')$ state, in which Φ is increased from 137.5° of the ground state to 180.0° of the excited state. This state can be describe as two distinct single-electron transition configurations 2a″ → 9a′ and 9a′ → 2a″ in C_s symmetry, which make the 9a′ and 2a″ orbitals degenerate. The geometry of the $2^1\Sigma^+$ excited state is linear, and it has a dominant leading configuration of $[\mathrm{core}](4\sigma)^2(5\sigma)^2(6\sigma)^2(7\sigma)^2(1\pi)^4(2\pi)^2$ with a coefficient of 0.936, where [core] denotes $(1\sigma)^2(2\sigma)^2(3\sigma)^2$.

The R_{CN} is elongated more severely for state $2^1A''$, in which it is elongated to 0.120 Å. This state can be described as two different single transition configurations, 1a″ → 2a″ and 8a′ → 9a′ with the coefficients −0.428 and 0.504. The 1a″ is mainly of π-type bonding character resulting from the interaction of the $2p_z$ of the atom N and C1. The 8a′ orbital is of π-type bonding character and mostly made up of $2p_x$ of the atom N, C1. The double electron transitions badly weaken the interactions of C1 and N atoms. The final optimized geometrical parameters calculated in this paper are $R_{CH} = 1.063$ Å, $R_{CC} = 1.350$ Å, $R_{CN} = 1.304$ Å, Ω = 168.4°, and Φ = 135.4°, respectively.

The $2^3A''$ can be seen as a single-electron transition configuration 8a′ → 9a′ with a coefficient of 0.821. For the single-electron transition, the electron is transferred from the N−C1 bonding orbital to a slight antibonding orbital of N−C2 and the bonding interaction between the N and C1 atoms is impaired.

TABLE 1: Optimized Structures (in Å and deg), Leading Configuration, CI Coefficient, Occupation, and Adiabatic Excitation Energies (T_a in eV) for the Ground State and Excited States of HCCN Calculated at the CASPT2//CASSCF Level of Theory, Using the aug-cc-PVTZ Basis Set

						configuration			
state	R_{CH} (Å)	R_{CC} (Å)	R_{CN} (Å)	Ω (deg)	Φ (deg)	coef	occupation[a]	$T_{a(CASSCF)}$ (eV)	$T_{a(CASPT2)}$ (eV)
X^3A''	1.063	1.372	1.184	175.6	137.5	−0.939	$(7a')^2(8a')^2(1a'')^2(9a')^\alpha(2a'')^\alpha$	0.000	0.000
$^1A'$	1.114	1.413	1.173	174.1	107.6	0.930	$(7a')^2(8a')^2(1a'')^2(9a')^2(2a'')^0$	0.702	0.738
$^1A''$	1.057	1.319	1.203	176.2	155.6	−0.940	$(7a')^2(8a')^2(1a'')^2(9a')^\alpha(2a'')^\beta$	1.365	0.932
$2^1\Sigma^+(2^1A')$	1.054	1.293	1.219	180.0	180.0	0.936	$(7\sigma)^2(1\pi)^4(2\pi)^2$	2.041	1.556
$2^1A''$	1.063	1.350	1.304	168.4	135.4	−0.435	$(7a')^2(8a')^2(1a'')^2(9a')^\alpha(2a'')^\beta$	3.822	3.315
						−0.428	$(7a')^2(8a')^2(1a'')^\beta(9a')^\alpha(2a'')^2$		
						0.504	$(7a')^2(8a')^\alpha(1a'')^2(9a')^2(2a'')^\beta$		
$2^3A''$	1.098	1.366	1.300	161.6	121.5	0.821	$(7a')^2(8a')^\alpha(1a'')^2(9a')^2(2a'')^\alpha$	4.071	3.579
$^3A'$	1.102	1.377	1.288	167.7	116.6	0.930	$(7a')^2(8a')^2(1a'')^\alpha(9a')^2(2a'')^\alpha$	4.204	3.896
$2^3A'$	1.080	1.322	1.296	173.2	144.8	0.448	$(7a')^2(8a')^2(1a'')^\alpha(9a')^2(2a'')^\alpha$	4.750	4.252
						0.833	$(7a')^2(8a')^\alpha(1a'')^2(9a')^2(2a'')^\alpha$		
$3^1A'$	1.099	1.403	1.305	119.6	129.4	0.341	$(7a')^2(8a')^\alpha(1a'')^2(9a')^2(2a'')^\beta$	5.307	4.824
						0.809	$(7a')^2(8a')^\alpha(1a'')^2(9a')^2(2a'')^\alpha(11a')^\beta$		
$3^1A''$	1.097	1.381	1.202	166.2	119.7	−0.904	$(7a')^\alpha(8a')^2(1a'')^2(9a')^2(2a'')^\beta$	5.487	5.074

[a] The occupation number represents the electronic number that is occupied in the active space. α represents a spin-up electron, β represents a spin-down electron, and 2 represents double occupied electrons. Every state has a common configuration $[core](4a')^2(5a')^2(6a')^2$ or $[core](4\sigma)^2(5\sigma)^2(6\sigma)^2$, which we will not present in the table.

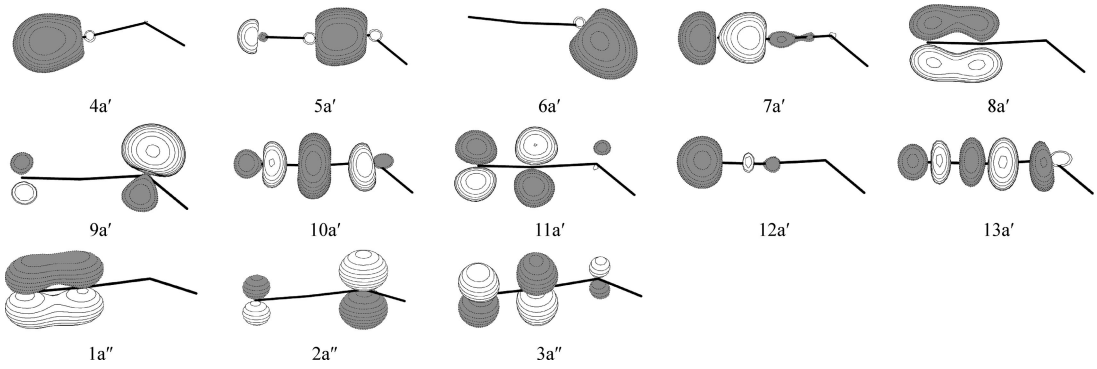

Figure 2. The plots of densities for a part of HCCN orbitals included in the active space.

So, the N−C bond is elongated 0.116 Å, the C−C bond is shortened 0.006 Å, the C−H bond is elongated 0.035 Å, the angle Ω is reduced 16.0°, and the angle Φ is decreased 5.7°, respectively.

The single-electron transition 1a″ → 9a′ in the $^3A'$ state, which has a leading configuration of $[core](4a')^2(5a')^2(6a')^2(7a')^2(8a')^2(1a'')^\alpha(9a')^2(2a'')^\alpha$, has a coefficient of 0.930. The electron is transferred from the 1a″ to the 9a′, which impaired the interaction of the π bonding of the 1a″. The geometrical data for this state are R_{CH} = 1.102 Å, R_{CC} = 1.377 Å, R_{CN} = 1.288 Å, Ω = 167.7°, and Φ = 116.6°.

For the $2^3A'$ state, it can be described as the 1a″ → 9a′ and 8a′ → 2a″ double electrons transitions. The transitions impaired the interaction of C1 and N atoms. Compared with the ground state, R_{CN} is elongated to 0.112 Å. The changes of the other geometrical parameters are not obvious.

All the bond lengths of the $3^1A'$ state are elongated because this state has two dominant leading configurations which can be described as single-electron transition 1a″ → 9a′ and 2a″ → 11a′ with coefficients of 0.341 and 0.809, respectively. From Figure 2, we found that 11a′ shows mainly dominant π^*(N−C1) orbital antibonding character. So, after the electron promotion, the R_{CN}, R_{CC}, and R_{CH} are elongated 0.036, 0.041, and 0.121 Å, and the bond angles Ω and Φ are decreased 56.0° and 8.1°, respectively.

The single-electron transition 7a′ → 9a′ results in the unparallel spin excited state $3^1A''$. The 7a′ orbital has mainly dominant σ(C1−N) bonding character. The single-electron transition impaired the interaction of N and C1 atoms. As compared with the ground state of HCCN, the R_{CH}, R_{CC}, and R_{CN} are elongated 0.034, 0.009, and 0.018 Å, and the Ω and Φ are decreased 9.4° and 17.8°, respectively.

TABLE 2: Vibration Frequencies for the Ground and Excited States of HCCN Calculated by MCLR[b]

	harmonic vibration frequency(cm^{-1})						
state	ν_1(a′)	ν_2(a′)	ν_3(a′)	ν_4(a′)	ν_5(a′)	ν_6(a″)	
X^3A''	3448.0	1949.9	1066.0	778.6	383.6	423.4	
exp[a]	3229.2	1734.9	1178.6				
$2^3A''$	3069.5	1687.5	1046.5	698.6	348.3	395.9	
$^3A'$	3033.7	1789.6	1036.9	810.4	446.6	424.7	
$2^3A'$	3262.4	1915.9	1109.5	476.6	93.1i	429.8	
$^1A'$	2931.4	2138.9	1099.9	992.3	425.6	324.0	
$2^1\Sigma^+(2^1A')$	3548.4	1897.6	1256.1	508.5	448.7	515.8	453.4
$3^1A'$	3104.9	1431.8	1255.5	1017.7	266.6	961.8	
$^1A''$	3546.4	1861.3	1202.4	465.7	350.4	443.8	
$2^1A''$	3449.4	1866.9	1048.8	720.8	371.4	420.9	
$3^1A''$	3080.6	2046.2	1076.4	783.0	506.5	482.7	

[a] ν_1 represents the HC stretch, ν_2 represents the CCN asym stretch, ν_3 represents the CCN sym stretch, ν_4 represents the CCN in-plane bend, ν_5 represents the HCC bend, and ν_6 represents the CCN out-of-plane bend. [b] Reference 35.

After the geometry optimizations, the frequency analyses are also performed. In Table 2, we list the harmonic vibration frequency values corresponding to six types of normal modes, in which ν_1 represents the HC stretch, ν_2 represents the CCN

TABLE 3: The CASPT2 *Tv* (Calculated at the Ground State Geometry of the HCCN Radical) Values and Oscillator Strengths (*f*) for the 11 States of the HCCN Caynocarbene Radical

state	transition	*Tv* (eV)	*f*
X^3A''	ground-state	0.000	ground state
$^1A'$		0.938	$<10^{-10}$
$^1A''$		1.113	$<10^{-10}$
$2^1A'$		2.329	$<10^{-10}$
$2^1A''$		3.850	$<10^{-10}$
$2^3A''$		4.179	0.014800
$^3A'$		4.395	0.000180
$33A''$	$7a' \rightarrow 9a'$	4.579	0.014300
$2^3A'$		4.727	0.000908
$3^3A'$	$1a'' \rightarrow 9a'$ $2a'' \rightarrow 11a'$ $8a' \rightarrow 2a''$	5.056	0.005970
$3^1A''$		5.274	$<10^{-10}$
$3^1A'$		5.397	$<10^{-10}$

asymmetry stretch, ν_3 represents the CCN symmetry stretch, ν_4 represents the CCN in-plane bend, ν_5 represents the HCC bend, and ν_6 represents the CCN out-of-plane bend. Available experimental frequency values in three modes of the ground state are listed in Table 2. The CASSCF harmonic frequencies we calculated show agreement with the experimental values. The $2^1\Sigma^+(2^1A')$ state as a linear excited molecular has seven vibrational modes, in which 453.4 represents the HCC bend. For the $2^3A'$ state, there is a small imaginary frequency 93.1i, which indicates that this state is unstable.

Absorption Spectra. The computed vertical excitation energies at the CASSPT2//CASSCF/aug-cc-pVTZ levels are listed in Table 3 together with the corresponding oscillator strengths. According to Franck−Condon theory, all of the vertical calculations are performed based on the equilibrium geometry of the neutral ground state.

The oscillator strengths for the transitions between the ground and excited states were calculated. To obtain a nonvanishing transition dipole moment, $\langle\psi_i|\{\hat{\mu}\}|\psi_j\rangle$, the direct product, $\Gamma_i \times \Gamma_\mu \times \Gamma_j$, must contain the totally symmetric irreducible representation. In the case of the C_s point group, $\Gamma_{\mu y}$ and $\Gamma_{\mu z}$ are A′ and the ground state symmetry is X^3A'', thus transitions into states of A″ symmetry are dipole allowed, and $\Gamma_{\mu x}$ is A″, thus transition into states of A′ symmetry are dipole allowed. Our calculated oscillator strengths reflect exactly there selection rules, oscillator strengths of transition into states $^1A'$, $2^1A'$, $3^1A'$, $^1A''$, $2^1A''$, and $3^1A''$ are above 10 orders of magnitude smaller than those for $2^3A''$, $3^3A''$, $^3A'$, $2^3A'$ and $3^3A'$. It also shows that transitions from the triplet state into triplet states are available. As shown in Table 3, the $X^3A'' \rightarrow 2^3A''$, $X^3A'' \rightarrow {}^3A''$, $X^3A'' \rightarrow 3^3A''$, $X^3A'' \rightarrow 2^3A'$, and $X^3A'' \rightarrow 3^3A'$ transitions calculated at 4.179, 4.395, 4.579, 4.727, and 5.056 eV have oscillator strengths of 0.014800, 0.000180, 0.014300, 0.000908, and 0.005970 respectively. Among these allowed transitions the energy of $X^3A'' \rightarrow 2^3A''$ is the lowest, due to the $8a' \rightarrow 9a'$ electronic promotion, which is the most intensive transition.

Aoki calculated the vertical excitation energies from the ground state to $^1A'$ and $^1A''$ excited states are 0.93 and 1.11 eV,[23] respectively, which agrees with our results.

Detachment Energies and State Characteristics of the $HCCN^-$ Anion. To further investigate the chemical properties of HCCN, the ground and excited states of $HCCN^-$ using the same basis sets and methods were also calculated. All of the states for experimental C_s symmetry equilibrium geometry that we obtained at the CASPT2//CASSCF level are summarized in Table 4, which contains energies and configuration information. Furthermore, we calculated the vertical electron affinity energy (VEA) and adiabatic electronic affinity (AEA).

1. Equilibrium Geometries of the $HCCN^-$ Anion. The lowest electronic state of the linear $HCCN^-$ anion has the degenerate electronic configurations $[\text{core}](4\sigma)^2(5\sigma)^2(6\sigma)^2(7\sigma)^2(1\pi)^4(2\pi_i)^2(2\pi_o)^\alpha$ ($^2\Pi$) and $[\text{core}](4\sigma)^2(5\sigma)^2(6\sigma)^2(7\sigma)^2(1\pi)^4(2\pi_i)^\alpha(2\pi_o)^2$ ($^2\Pi$), where π_i and π_o stand for the in-plane and out-of-plane π molecular orbitals. This linear configuration of $HCCN^-$ presents two distinct imaginary vibrational frequencies, 882.9i (in-plane) and 371.3i cm^{-1} (out-of-plane) with the CASSCF method, along the HCC bending coordinates. According to the analysis of linear triatomic Renner−Teller molecules by Lee et al.,[40] the $HCCN^-$ anion is classified as a type D Renner−Teller molecule. Following the eigenvector of the in-plane imaginary bending frequency, the $^2A''$ component of the $^2\Pi$ state is stabilized to a nonlinear equilibrium structure of the ground state (X^2A''), and following the eigenvector of the out-of-plane imaginary bending frequency, the $^2A'$ component is also stabilized to nonlinear equilibrium geometry. Since the magnitude of the imaginary bending frequency is larger for the in-plane motion, the distortion from linearity is expected to be greater for the X^2A'' state. The X^2A'' ground state of $HCCN^-$ is strongly bent ($\Phi = 109.3°$) and exhibits a barrier to linearity of 0.575 eV. The excited $^2A'$ negative ion state corresponds to an obtuse angle structure ($\Phi = 143.3°$), but could be termed as quasilinear, since the barrier to linearity calculates to be only 0.006 eV, which is slightly lower than the results of Josef.[32]

The adiabatic excitation energies, which had never been reported, and the results were summarized in Table 4. The X^2A'' ground state has a dominant leading configuration $[\text{core}](4a')^2(5a')^2(6a')^2(7a')^2(8a')^2(1a'')^2(9a')^2(2a'')^\alpha$ with a coefficient 0.946. As compared to the HCCN neutral radical's electronic structure, this state is mainly created by adding a single electron to the slight antibonding 9a′ orbital of the X^3A'' state of HCCN. This electron's addition increased the interaction of the antibonding of 9a′, which makes the bond lengths elongated in the $HCCN^-$ anion. Nimlos et al.[29] calculated geometrical parameters ($R_{CH} = 1.113$ Å, $R_{CC} = 1.402$ Å, $R_{CN} = 1.193$ Å, $\Omega = 173.5°$, and $\Phi = 106.7°$) were quite close to ours.

As shown in Table 4, the absolute value of coefficient for the X^2A'', $^2A'$, $^4A''$, $^4A'$, and $^4\Sigma^+(2^4A'')$ of the HCCN leading configurations is above 0.90, indicating a single-reference character of the respective states. The value of the $2^2A'$ is 0.869, which indicates a low multireference character. The other states show obvious multireference characters. According to Figure 2 and Table 4, the change of structures can be reasonably explained and we will not discuss it in detail here. The calculated harmonic frequencies for ionic states are listed in the Supporting Information (Table S1). All of the frequencies are real, and the optimized electronic states are confirmed to be stable except for the $2^2A'$ state. For the $2^2A'$ state, there is an imaginary frequency 474.3i, which indicates that this state is unstable. Furthermore, our calculated harmonic frequency of 2845.5, 1975.0, 1031.9, 1001.5, 493.7, and 494.9 cm^{-1} for the ground state X^2A'' also agreed well with the theoretical results of 2926, 1948, 1072, 947, 512, and 508 cm^{-1} calculated by Nimlos et.[29]

2. Detachment Energies. The PES of the anion represents transitions from the electronic ground state of the anion to the ground and excited states of the neutral molecule. As mention above, the ground state geometry of the anion is used for the vertical detachment energetic calculation. Taking into account the further correlation effects, the CASPT2 method is here used to obtain more reliable energies.

TABLE 4: Optimized Structures (in Å and deg), Leading Configuration, CI Coefficient, Occupation, and Adiabatic Excitation Energies (T_a in eV) for the Ground State and Excited States of $HCCN^-$ Calculated at the CASPT2//CASSCF Level of Theory, Using the aug-cc-PVTZ Basis Set

						configuration			
state	R_{CH} (Å)	R_{CC} (Å)	R_{CN} (Å)	Ω (deg)	Φ (deg)	coeff	occupation[a]	$T_{a(CASSCF)}$ (eV)	$T_{a(CASPT2)}$ (eV)
$^2A''$	1.116	1.397	1.192	174.9	109.3	0.946	$(7a')^2(8a')^2(1a'')^2(9a')^2(2a'')^\alpha$	0.000	0.000
$^2A'$	1.080	1.340	1.216	176.3	143.3	0.944	$(7a')^2(8a')^2(1a'')^2(9a')^\alpha(2a'')^2$	0.397	0.569
$^4A''$	1.067	1.368	1.179	175.1	136.7	0.950	$(7a')^2(8a')^2(1a'')^2(9a')^\alpha(2a'')^\alpha(10a')^\alpha$	1.316	2.317
$2^2A''$	1.083	1.394	1.310	169.7	114.6	−0.843	$(7a')^2(8a')^2(1a'')^\alpha(9a')^2(2a'')^2$	3.959	3.855
						0.322	$(7a')^2(8a')^2(1a'')^2(9a')^2(3a'')^\alpha$		
$2^2A'$	1.077	1.357	1.311	169.6	119.6	0.869	$(7a')^2(8a')^\alpha(1a'')^2(9a')^2(2a'')^2$	4.021	3.880
$^4A'$	1.080	1.351	1.163	176.4	137.2	−0.964	$(7a')^2(8a')^2(1a'')^2(9a')^\alpha(2a'')^\alpha(3a'')^\alpha$	4.259	4.000
$^4\Sigma^+$ ($^4A''$)	1.056	1.305	1.312	180.0	180.0	0.941	$(7\sigma)^2(1\pi)^2(1\pi)^\alpha(2\pi)^2(2\pi)^\alpha(1\pi^*)^\alpha$	5.763	6.323
$2^4A'$	1.058	1.310	1.309	174.5	157.6	0.573	$(7a')^2(8a')^2(1a'')^2(9a')^\alpha(2a'')^\alpha(3a'')^\alpha$	5.945	6.528
						−0.763	$(7a')^2(8a')^\alpha(1a'')^2(9a')^\alpha(2a'')^2(10a')^\alpha$		

[a] The occupation number represents the electronic number that is occupied in the active space. α represents a spin-up electron, β represents a spin-down electron, and 2 represents double occupied electrons. Every state has a common configuration $[core](4a')^2(5a')^2(6a')^2$ or $[core](4\sigma)^2(5\sigma)^2(6\sigma)^2$, which we will not present in the table.

TABLE 5: The Calculated Vertical (VDE, eV) and Adiabatic (ADE, eV) Detachment Energies of $HCCN^-$ and the Corresponding Reported Experimental DE

		ADE	
state	VDE	calcd	expt[a]
X^3A''	2.210	1.768	2.014
$^1A'$	2.505	2.507	2.518 ± 0.008
$^1A''$	3.458	2.700	
$2^1A'$	5.362	3.324	
$2^1A''$	5.698	5.084	
$2^3A''$	5.779	5.348	
$^3A'$	6.016	5.665	
$2^3A'$	6.451	6.021	
$3^3A''$	6.777		
$3^1A''$	6.927	6.843	
$3^1A'$	7.092	6.592	
$3^3A'$	7.399		

[a] Reference 30.

The first detachment energy of the experimental value corresponds to the X^3A'' ground state of the neutral radical. Comparing the leading configurations of the ground state between the anion and radical, the photoelectron transition, HCCN (X^3A'') ″ $HCCN^-$ (X^2A''), results from detachment of one electron of the 9a′ orbtial. The first ADE and VDE calculated are 1.768 and 2.210 eV at the CASPT2 level, respectively, which is slightly lower than the experimental ADE value of 2.014 eV. The energy separation between ADE and VDE is 0.442 eV, because the 9a′ orbital is not an absolutely nonbonding orbital but has little part of the N−C2 interaction character, as described above.

As shown in Table 1, the $^1A'$ is the first excited state of the HCCN. The HCCN ($^1A'$) ← $HCCN^-$ (X^2A'') transition results from ejection of one electron of the 2a″ orbital. The calculated ADE and VDE of the $^1A'$ are 2.507 and 2.505 eV at the CASPT2 level, respectively, which agree well with the experimental ADE values of 2.518 ± 0.008 eV. As shown in Table 5, the ADEs of $^1A''$, $2^1A'$, $2^1A''$, $2^3A''$, $^3A'$, $2^3A'$, and $3^1A''$ states are 2.700, 3.324, 5.084, 5.348, 5.665, 6.021, and 6.843 eV, and their VDEs are 3.458, 5.698, 5.779, 6.016, 6.777, 7.092, and 6.927 eV, respectively. However, when a photodetachment apparatus is used for the negative ion photoelectron spectra, these values were not observed. We hope further precise experiments can find them.

Ionization Energies and State Characteristics of the $HCCN^+$ Cation. Although there are no experimental data available for the structure of the $HCCN^+$ cation, we here discussed its geometric structures for both the ground and excited states because $HCCN^+$ is produced from the photoelectron ionization of the HCCN radical. A total of six ionic states of the $HCCN^+$ cation are optimized adiabatically, and the frequency analyses are also performed at the CASPT2//CASSCF level. The geometric parameters and the configuration information are listed in Table 6, and the harmonic frequencies can be found in the Supporting Information (Table S2). Furthermore, the vertical ionization energies (VIP) and adiabatic ionization energies (AIP) were calculated.

1. Equilibrium Geometries of the $HCCN^+$ Anion. According to our calculations, the bent ground state, X^2A', and the linear first excited state, $^2\Pi(^2A'')$, form a Renner−Teller pair derived from a linear $^2\Pi$ configuration. For the linear configuration, $HCCN^+$ possesses a lowest $^2\Pi$ electronic state and displays one real (858.4) and one imaginary vibrational frequency (329.8i) along the HCC bending coordinates. The eigenvector of the imaginary vibrational frequency leads to a trans-planar bent structure for the electronic state (X^2A'). The component of the $^2\Pi$ state with the real bending vibrational frequency is assigned to the $^2\Pi(^2A'')$ state. On the basis of adiabatic energies, we can see that the energy gap of the X^2A' and $^2\Pi(^2A'')$ states is only 0.009 eV, which indicates that the Renner−Teller pair degenerate in the linear geometry. Similarly, when displaced along the HCC bending coordinate, the $2^2\Pi$ state splits into $2'A'$ and $2^2\Pi(^2A'')$, and the $^4\Pi$ state splits into 4A″ and $^4\Pi(^4A')$ components by the Renner−Teller effect.

The adiabatic excitations were calculated, which had never been reported, and the results were summarized in Table 6. The ground state X^2A' has a leading configuration $[core](4a')^2(5a')^2(6a')^2(7a')^2(8a')^2(1a'')^2(9a')^\alpha(2a'')^0$ with a coefficient of −0.918. The $^2\Pi(^2A'')$ state has a dominant leading configuration $[core](4\sigma)^2(5\sigma)^2(6\sigma)^2(7\sigma)^2(1\pi)^4(2\pi)^0(2\pi)^\alpha$ with a coefficient of 0.918. The X^2A' and $^2\Pi(^2A'')$ states of the $HCCN^+$ cation can be described as deleting an electron from the singly occupied 2a″ and 9a′ orbital of the X^3A'' ground state of HCCN, respectively. As shown in Table 6, the absolute values of the coefficient for the X^2A', $^2\Pi(^2A'')$, $^4\Pi(^4A')$, and $^4A'$ of the $HCCN^+$ leading configurations are above 0.90, indicating a single-reference character of the respective states. The other states show obviously multireference characters. The geometrical structures of the ground and excited states of $HCCN^+$ can be reasonably explained according to Table 6 and Figure 2 and we do not discuss these results in detail here.

TABLE 6: Optimized Structures (in Å and deg), Leading Configuration, CI Coefficient, Occupation, and Adiabatic Excitation Energies (T_a in eV) for the Ground State and Excited States of $HCCN^+$ Calculated at the CASPT2//CASSCF Level of Theory, Using the aug-cc-PVTZ Basis Set

						configuration			
state	R_{CH} (Å)	R_{CC} (Å)	R_{CN} (Å)	Ω (deg)	Φ (deg)	coeff.	occupation[a]	$T_{a(CASSCF)}$ (eV)	$T_{a(caspt2)}$ (eV)
X^2A'	1.095	1.317	1.212	174.1	152.7	−0.918	$(7a')^2(8a')^2(1a'')^2(9a')^\alpha(2a'')^0$	0.000	0.000
$^2\Pi(^2A'')$	1.092	1.300	1.219	180.0	180.0	0.918	$(7\sigma)^2(1\pi)^2(1\pi)^2(2\pi)^0(2\pi)^\alpha$	0.018	0.009
$^4\Pi(^4A')$	1.090	1.311	1.313	180.0	180.0	0.934	$(7\sigma)^2(1\pi)^2(1\pi)^\alpha(2\pi)^\alpha(2\pi)^\alpha$	2.508	2.430
$2^2A'$	1.098	1.362	1.290	167.8	134.5	−0.575	$(7a')^2(8a')^2(1a'')^2(9a')^\alpha(2a'')^0$	3.105	2.910
						−0.547	$(7a')^2(8a')^\alpha(1a'')^\beta(9a')^2(2a'')^\alpha$		
$2^2\Pi(2^2A'')$	1.089	1.323	1.304	180.0	180.0	0.540	$(7\sigma)^2(1\pi)^2(1\pi)^\alpha(2\pi)^0(2\pi)^2$	3.205	2.963
						−0.672	$(7\sigma)^2(1\pi)^\alpha(1\pi)^2(2\pi)^\alpha(2\pi)^\beta$		
$^4A''$	1.101	1.363	1.237	160.8	140.4	0.923	$(7a')^2(8a')^\alpha(1a'')^2(9a')^\alpha(2a'')^\alpha$	3.193	6.104

[a] The occupation number represents the electronic number that is occupied in the active space. α represents a spin-up electron, β represents a spin-down electron, and 2 represents double occupied electrons. Every state has a common configuration $[core](4a')^2(5a')^2(6a')^2$ or $[core](4\sigma)^2(5\sigma)^2(6\sigma)^2$, which we will not present in the table.

TABLE 7: The Calculated Vertical and Adiabatic IPs (eV) of HCCN

state	AIPs	VIPs
X^2A'	10.503	10.652
$^2A''$	10.513	11.329
$^4A''$	16.607	13.183
$^4A'$	12.933	13.320
$2^2A'$	13.413	13.739
$2^2A''$	13.467	13.976

2. Ionization Energies. There are no experimental and calculated data available for the information of the $HCCN^+$ cation. The first ionization potential of the HCCN cyanocarbene corresponds to the X^2A' state of the $HCCN^+$ cation. Comparing the ground state configurations of the HCCN shown in Table 1 with those of the cation shown in Table 5, we can see that this ionization is mainly generated by removing the 2a″ electron from the dominant leading configuration of $HCCN(X^3A'')$. The calculated adiabatic ionization energies and vertical ionization energies were summarized in Table 7. As can be seen from Table 7, the calculated first AIP and VIP are 10.503 and 10.652 eV, respectively, and the energy separation between them is 0.152 eV, which means that 2a″ of the HCCN is not nonbonding orbitals but has a small degree of N−C2 antibonding interaction, as discussed above.

Conclusions

The present work investigated the ground state and low-lying excited states of cyanocarbene HCCN, its anion $HCCN^-$, and cation $HCCN^+$, using the CASPT2//CASSCF level with the aug-cc-pVTZ basis set. The electronic configurations are used to explain the geometrical alteration in detail. We have presented results from a fully correlated ab initio investigation of the electronic spectrum of HCCN neutral radical by means of using the CASPT2 method, a well-established procedure for accurate calculations of electronic spectra of molecules. The five low-lying triplet valence excited states ($2^3A''$, $3^3A''$, $^3A'$, $2^3A'$, and $3^3A'$) are located at 4.179, 4.395, 4.579, 4.727, and 5.056 eV with significant oscillator strength. Among the allowed transitions the energy of $X^3A'' \rightarrow 2^3A''$ is the lowest, which is the most intensive transition.

On the basis of the corresponding results, the PES of the HCCN radical and $HCCN^-$ anion are assigned. The vertical and adiabatic ionization energies are assigned to six ionic states at the CASPT2 level. The computed first VIP and AIP are 10.652 and 10.513 eV, respectively.

The vertical detachment energy VDE in a wide range of 2.210−7.399 eV is assigned to a total 12 neutral states at the CASPT2 level. The ten detachment energies are also confirmed at the CASPT2 level adiabatically. For the PES of the anion, the first VDE and ADE calculated are 1.568 and 1.768 eV, which are comparable with the experimental data of 2.003 ± 0.014 eV. The calculated VDE and ADE of the $^1A'$ state are 2.305 and 2.507 eV, respectively, which agree well with the ADE values of 2.518 ± 0.008 eV in the experiment.

Supporting Information Available: Table S1 and Table S2 containing the frequencies of the ground and excited states for $HCCN^-$ and $HCCN^+$. This material is available free of charge via the Internet at http://pubs.acs.org.

References and Notes

(1) *Advances in Carbene Chemistry*; Brinker, U. H., Ed.; Jai Press: Greenwich and Stamford, 1994 and 1998; Vols. 1 and 2.
(2) Bourissou, D.; Guerret, O.; Gabbaı, F. P.; Bertrand, G. *Chem. Rev.* **2000**, *100*, 39.
(3) Yung, Y. L.; Allen, M.; Pinto, J. P. *Astrophys. J. Suppl* **1984**, *55*, 465.
(4) Yung, Y. *Icarus* **1987**, *72*, 468.
(5) Bernheim, R. A.; Kempf, R. J.; Humer, P. W.; Skell, P. S. *J. Chem. Phys.* **1964**, *41*, 1156.
(6) Wasserman, E.; Yager, W. A.; Kuck, V. J. *Chem. Phys. Lett.* **1970**, *7*, 409.
(7) Dendramis, A.; Leroi, G. E. *J. Chem. Phys.* **1977**, *66*, 4334.
(8) Saito, S.; Endo, Y.; Hirota, E. *J. Chem. Phys.* **1984**, *80*, 1427.
(9) Brown, F. X.; Saito, S.; Yamamoto, S. *J. Mol. Spectrosc.* **1990**, *143*, 203.
(10) Morter, C. L.; Farhat, S. K.; Curl, R. F. *Chem. Phys. Lett.* **1993**, *207*, 153.
(11) McCarthy, M. C.; Gottlieb, C. A.; Cooksy, A. L.; Thaddeus, P. *J. Chem. Phys.* **1995**, *103*, 7779.
(12) Miller, C. E.; Eckhoff, W. C.; Curl, R. F. *J. Mol. Struct.* **1995**, *352−353*, 435.
(13) Sun, F.; Kosterev, A.; Scott, G.; Litosh, V.; Curl, R. F. *J. Chem. Phys.* **1998**, *109*, 8851.
(14) Han, J.; Hung, P. Y.; DeSain, J.; Jones, W. E.; Curl, R. F. *J. Mol. Spectrosc.* **1999**, *198*, 421.
(15) Hung, P. Y.; Sun, F.; Hunt, N. T.; Burns, L. A.; Curl, R. F. *J. Chem. Phys.* **2001**, *115*, 9331.
(16) Allen, M. D.; Evenson, K. M.; Brown, J. M. *J. Mol. Spectrosc.* **2001**, *209*, 143.
(17) Harrison, J. F.; Dendramis, A.; Leroi, G. E. *J. Am. Chem. Soc.* **1978**, *100*, 4352.
(18) Zandler, M. E.; Goddard, J. D.; Schaefer, H. F. *J. Am. Chem. Soc.* **1979**, *101*, 1072.
(19) Kim, K. S.; Schaefer, H. F.; Radom, L.; Pople, J. A.; Binkley, J. S. *J. Am. Chem. Soc.* **1983**, *105*, 4148.
(20) Rice, J. E.; Schaefer, H. F. *J. Chem. Phys.* **1987**, *86*, 7051.
(21) Malmqvist, P.-Å.; Lindh, R.; Roos, B. O.; Ross, S. *Theor. Chim. Acta* **1988**, *73*, 155.
(22) Seidl, E. T.; Schaefer, H. F. *J. Chem. Phys.* **1992**, *96*, 4449.
(23) Aoki, K.; Ikuta, S.; Nomura, O. *J. Chem. Phys.* **1993**, *99*, 3809.
(24) Kellogg, C. B.; Galbraith, J. M.; Fowler, J. E.; Schaefer, H. F., III. *J. Chem. Phys.* **1994**, *101*, 430.
(25) Francisco, J. S. *Chem. Phys. Lett.* **1994**, *230*, 372.

(26) Goldberg, N.; Fiedler, A.; Schwarz, H. *J. Phys. Chem.* **1995**, *99*, 15327.
(27) Maier, G.; Raisenauer, H. P.; Rademacher, K. *Chem. Eur. J.* **1998**, *4*, 1957.
(28) Koput, J. *J. Phys. Chem. A* **2002**, *106*, 6183.
(29) Nimlos, M.; Davico, G.; Wenthold, P.; Lineberger, W.; Blanksby, S.; Hadad, C.; Peterson, G.; Ellison, G. *J. Chem. Phys.* **2002**, *117*, 4323.
(30) Poutsma, J. C.; Upshaw, S. D.; Squires, R. R.; Wenthold, P. G. *J. Phys. Chem. A* **2002**, *106*, 1067.
(31) Koput, J. *J. Phys. Chem. A* **2003**, *107*, 4717.
(32) Kalcher, J. *Chem. Phys. Lett.* **2005**, *403*, 146.
(33) Andersson, K.; et al. *LCAS*, version 6.0; University of Lund: Sweden, 2004.
(34) Herzberg, G. *Proc. R. Soc. London, Ser. A* **1966**, *295*, 106.
(35) McKellar, A. R. W.; Bunker, P. R.; Sears, T. J.; Evenson, K. M.; Saykally, R. J.; Langhoff, S. R. *J. Chem. Phys.* **1983**, *79*, 5251.
(36) McKellar, A. R. W.; Bunker, P. R.; Sears, T. J.; Evenson, K. M.; Langhoff, S. R. *Bull. Soc. Chim. Belg.* **1983**, *92*, 499.
(37) Bunker, P. R.; Sears, T. J.; McKellar, A. R. W.; Evenson, K. M.; Lovas, F. J. *J. Chem. Phys.* **1983**, *79*, 1211.
(38) Hartland, G. V.; Qin, D.; Dai, H.-L. *J. Chem. Phys.* **1995**, *102*, 6641.
(39) NIST Chemistry WebBook edited by Linstrom, P. J., and Mallard, W. G. http://webbook.nist.gov/chemistry/(2005).
(40) Lee, T. J.; Fox, D. J.; Schacfer, H. F., III.; Pitzer, R. M. *J. Chem. Phys.* **1984**, *81*, 356.

JP8070663